The Effect of Very High Hydraulic Pressure on the Permeability and Salt Rejection of Reverse Osmosis Membranes

by

Dillon James McConnon

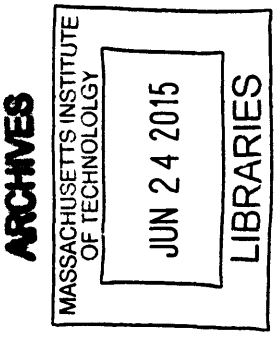

Submitted to the Department of Mechanical Engineering
in partial fulfillment of the requirements for the degree of

Bachelor of Science in Mechanical Engineering

at the

MASSACHUSETTS INSTITUTE OF TECHNOLOGY

June 2015

Author ..... Signature redacted
Department of Mechanical Engineering
May 8, 2015

Certified by ..... Signature redacted
Lallit Anand
Warren and Towneley Rohsenow Professor of Mechanical Engineering
Thesis Supervisor

Accepted by ..... Signature redacted
Anette Hosoi
Professor of Mechanical Engineering, Undergraduate Officer

The Effect of Very High Hydraulic Pressure on the Permeability and Salt Rejection of Reverse Osmosis Membranes

by

Dillon James McConnon

Submitted to the Department of Mechanical Engineering
on May 8, 2015, in partial fulfillment of the
requirements for the degree of
Bachelor of Science in Mechanical Engineering

Abstract

A stirred-cell reverse osmosis setup was used to demonstrate that a seawater reverse osmosis membrane can maintain excellent rejection at pressures as high as 172 bar. However, it was also demonstrated that there was a significant drop in permeability at high pressures - likely due to membrane compaction. A simple visco-elastic model was shown to be able to model the overall shape of the permeability curve in time. However, this model does not match the data well when pressure is removed and then reapplied. From the perspective of membrane performance, RO is feasible at high pressures but distinct challenges are presented by reduced permeability and increased variability in flux.

Thesis Supervisor: Lallit Anand
Title: Warren and Towneley Rohsenow Professor of Mechanical Engineering

Acknowledgments

I wish to express my appreciation to Professor Anand for advising me through my bachelor degree at MIT and for providing me research to conduct my thesis. I wish to express my appreciation also to Dr. McGovern whose patience and guidance were indispensable in the creation of this thesis.

I would also like to thank my friends and family for supporting me through my education. My parents' constant support and emphasis on education led me to college and MIT, and my friends helped get me through the stress of these four years here.

Contents

List of Figures

List of Tables

Chapter 1

Background

Thin film composite membranes, the seawater reverse osmosis membrane studied here, are a composite material made of three distinct layers - a porous fabric, a polysulfone support layer and a salt-rejection polyamide layer, known as the active layer. The active layer is the thinnest layer ($\sim$ 200 nm thick) and sits on top of the polysulfone layer. There is concern that high pressures applied to the active layer could cause tearing and lead to a decrease in ability to reject salt.

The study of thin film composite membranes, and their respective permeabilities, are important because of their use in separating solutes from solution. Widely used applications include seawater desalination and juice concentration [1]. In both desalination and juice concentration a pressure is applied to the solution that is being filtered by the membrane. In the case of desalination, the permeate (pure water) is generally the product, while in juice concentration the leftover feed (concentrate) is the product. In Figures 1-1 and 1-2 the osmotic pressure increases for different salinities and juice concentrations, respectively, is shown.

It is seen that as the concentration or salinity goes up, the needed pressure to overcome osmotic pressure goes up nearly linearly. If RO was able to be operated at higher pressures, RO could replace vapour compression systems that operate currently in juice concentration [3], which could also lead to a reduction in energy consumption. Using RO could lead to an increase in quality of the concentrate, as the heat from the vapour compression system cause an undesirable change in the concentrate's sensory

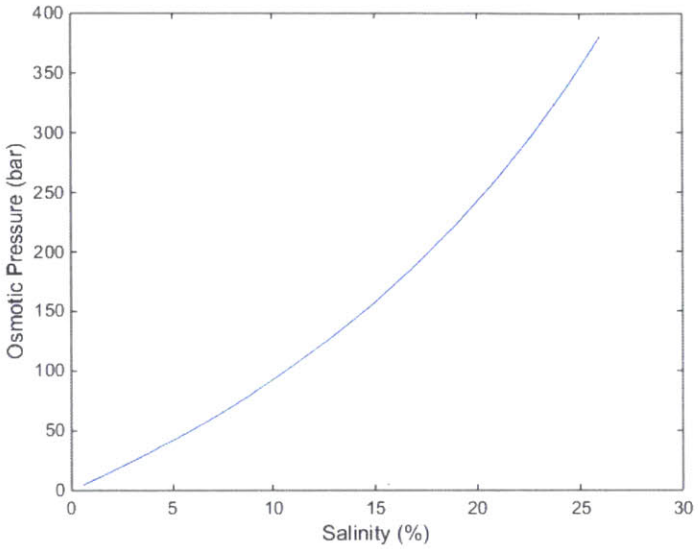

Figure 1-1: Graph of percent salinity versus osmotic pressure [5]. 3% salinity is the typical sea water salinity, while 26% is the saturation limit of NaCl in water.

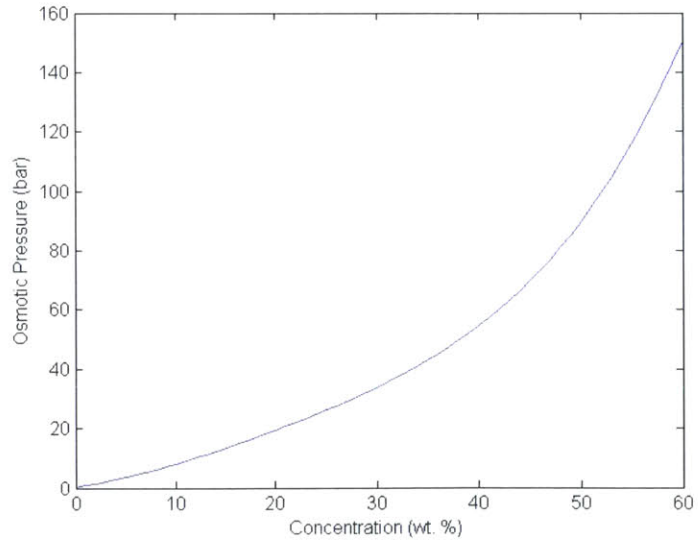

Figure 1-2: Graph of concentration of sucrose in applie juice versus osmotic pressure [6]. 15% solids is the starting concentration of apple juice, 60% solids represents concentrating the juice by 4.

properties. For desalination, operations could desalinate higher salinity waters and thus replace energy intensive vapour compression systems used currently [4], which would lead to a significant reduction in energy consumption.

Chapter 2

Introduction

Using a dead-end stirred cell it is demonstrated that seawater reverse osmosis (RO) membranes can reject salt effectively even when operating at 172 bar. Permeability of the membrane at this pressure, however, is 50% of its permeability at 34.5 bar. The membranes have a variable permeability in time, which can be modeled using a visco-elastic model.

These results are significant as they show that reverse osmosis membranes are effective, from the perspective of salt rejection, at pressures up to 172 bar. The results also show that the loss of permeability of the membrane can be predicted using a visco-elastic model.

One application of relevance to high pressure reverse osmosis systems is the purification of waters in the oil and gas industry, where certain highly saline waste water streams require purification. The use of reverse osmosis, which is by far the most energy efficient desalination technology for seawater desalination, is particularly interesting given the poor energy efficiency of the thermal technologies currently employed for the desalination of highly saline waters [4]. If feasible, high salinity reverse osmosis systems could potentially achieve significant reductions in energy consumption relative to mechanical vapour compression systems.

Another application of relevance to high pressure reverse osmosis systems is the concentration of juices and other liquids in the beverage industry [1]. The concentration of juices is typically done using mechanical vapour compression [3]. The

utilization of RO membranes for this process is of interest because of its lower energy usage [4] and its ability to be done at room temperature, which changes the taste properties of the concentrate less than the high temperatures of vapour compression [3].

Of relevance to the feasibility and usability of RO membranes is whether RO membranes can perform satisfactorily, in terms of salt rejection and permeability, at high pressures, and whether these results can be predicted. Previous studies on the effect of hydraulic pressure on thin film composite polyamide membranes have explored the possible visco-elastic models that can be used to model reverse osmosis membranes [8]. However, these studies have only looked at pressures in nano-filtration membranes up to 50 bar [9],[8] and 69 bar for thin film composite membranes [10]. One study looked at pressures up to 138 bar [7] but this study did not explore a model for their data. Determining the permeability of thin film composite membranes over longer periods of time (9 hours or more) at high pressure is essential for determining the feasibility of reverse osmosis membranes in high salinity applications. It is also important in determining a first - order approximation of the throughput, which is essential in the initial design of any high salinity system using reverse osmosis.

Chapter 3

Methods

These next sections describe how the experiments were set up, how they were run, and how the data was analyzed in order to track permeability and track salt passage with time. For these experiments three distinct tests were completed (each at a different pressure, 34.5 bar, 103.4 bar and 172.4 bar), repeated with three different membrane samples (trials) to get a mean and standard deviation of the data. The tests were run for 9 hours and had 3 different phases.

The phases are, in order:

1. Initial Salt Passage Phase
2. Permeability Testing Phase
3. Final Salt Passage Phase

The initial and final salt passage phases were added into the trial in order to gauge the effectiveness of the membrane at rejecting salt. The initial phase was used to determine whether the test could continue by measuring the salt passage. The maximum salt passage (defined as conductivity in permeate divided by conductivity in feed) was set at 3%. The final salt passage phase was to gauge the effectiveness of the membrane at the end of the trial. The long-term permeability phases' purpose was to give the membrane exposure to pressure for a long period of time so that the effects of this could be seen. In Tables 3.1 through 3.3 the detailed steps and times

for each test are recorded. There are multiple permeability steps due to the limited volume of the stirred cell (300 mL).

Phase	Initial Salt Rejection 1 (ISR1)	Initial Salt Rejection 2 (ISR2)	Feed Replacement (FR)	Permeability 1 (P1)	Feed Refill (FF)	Permeability 2 (P2)	Feed Replacement (FR)	Final Salt Rejection 1 (FSR1)	Final Salt Rejection 2 (FSR2)
Duration	30 min	15 min	8 min	3 hr 6 min	8 min	4 hr	8 min	30 min	15 min
Pressure	On	On	Off	On	Off	On	Off	On	On
Feed Salinity	1 g/L	>1 g/L	N/A	DI Water	N/A	DI Water	N/A	1 g/L	>1 g/L

Table 3.1: Chart for different phases of the 34.5 bar test. The above phases were repeated for three separate trials.

Phase	Initial Salt Rejection 1 (ISR1)	Initial Salt Rejection 2 (ISR2)	Feed Replacement (FR)	Permeability 1 (P1)	Feed Refill (FF)	Permeability 2 (P2)	Feed Refill (FF)	Permeability 3 (P3)	Feed Refill (FF)	Permeability 4 (P4)	Feed Replacement (FR)	Final Salt Rejection 1 (FSR1)	Final Salt Rejection 2 (FSR2)
Duration	30 min	15 min	8 min	1 hr 25 min	8 min	1 hr 25 min	8 min	2 hr	8 min	2 hr	8 min	30 min	15 min
Pressure	On	On	Off	On	Off	On	Off	On	Off	On	Off	On	On
Feed Salinity	1 g/L	>1 g/L	N/A	DI Water	N/A	DI Water	N/A	DI Water	N/A	DI Water	N/A	1 g/L	>1 g/L

Table 3.2: Chart for different phases of the 103.4 bar test. The above phases were repeated for three separate trials.

Phase	Initial Salt Rejection 1 (ISR1)	Initial Salt Rejection 2 (ISR2)	Feed Replacement (FR)	Permeability 1 (P1)	Feed Refill (FF)	Permeability 2 (P2)	Feed Refill (FF)	Permeability 3 (P3)	Feed Refill (FF)	Permeability 4 (P4)	Feed Replacement (FR)	Final Salt Rejection 1 (FSR1)	Final Salt Rejection 2 (FSR2)
Duration	30 min	15 min	8 min	1 hr 25 min	8 min	1 hr 25 min	8 min	2 hr	8 min	2 hr	8 min	30 min	15 min
Pressure	On	On	Off	On	Off	On	Off	On	Off	On	Off	On	On
Feed Salinity	1 g/L	>1 g/L	N/A	DI Water	N/A	DI Water	N/A	DI Water	N/A	DI Water	N/A	1 g/L	>1 g/L

Table 3.3: Chart for different phases of the 172.4 bar test. The above phases were repeated for three separate trials.

3.1 Experimental Setup

In this experiment, a dead-end stirred cell (HP4750X; Sterlitech, Washington, USA) was used. The cell is made of stainless steel and withstands pressures of up to 172 bar. Inside the cell a stirring bar can be suspended without making contact on the membrane. The membrane is secured against an EPDM O-ring. Before each trial, the stirred-cell was washed with soapy water and dried with a paper towel. For each trial a new EPDM o-ring was used and wetted with de-ionised water (DI water, McMaster-Car, New Jersey, USA).

The porous stainless steel metal backing for the membranes was used as a template to cut membranes. The membranes used in this experiment are SWC membranes (Hydranautics, California, USA) were stored in a solution of 0.1% by weight sodium bisulfite. The membranes were cut using standard paper scissors and rinsed twice in DI water and the loaded into the stirred cell.

At this point the salt solution for the salt passage phases were made. A precision scale (ML203E; Mettler Toledo, Billerica, MA, USA) was used to measure 0.3 g of sodium chloride (NaCl) salt. 300 mL of deionised water was added and the solution was mixed using a stirring plate. The solution was then poured into the stirred cell and the stirrer was placed in. The solution conductivity was measured and recorded. The speed of the stirrer was set to 500 rpm and the lid to the stirred cell was closed. The precision scale was setup under the output spigot of the stirred cell with a collection cup. This collected and recorded mass data of the cup every 5 seconds, which was later converted into a flux measurement.

3.1.1 Experimental Setup Validation

In order to ensure the process which we mounted the membrane into the cell worked correctly, a number of preliminary salt passage tests were conducted. For each test, a different membrane and a different o-ring was used. Once the procedure was thought to be good 3 sodium sulfate salt passage tests were conducted and 3 sodium chloride salt passage tests were conducted. Both solutions were at 1% by weight. Salt passage

tests involved placing the membrane in a 34.5 bar pressure for 30 minutes, then replacing the permeate cup with a new cup. After 15 more minutes the test was stopped and the conductivity was measured in the permeate. The percent passage was approximated by measuring the conductivities:

$$SP_a = S_p/S_{f,o} \approx k_p/k_{f,o} \tag{3.1}$$

where S_p is the permeate salinity, $S_{f,o}$ is the initial salinity of the feed, k_p is the conductivity of the permeate, and $k_{f,o}$ is the initial conductivity of the feed.

These tests produced an average of 1.33% salt passage for the sodium sulfate and 4.08% salt passage for the sodium chloride. This is precisely what we expected for a successful run because salt passage for sodium sulfate through a thin film composite membrane is much lower than sodium chloride for well executed tests [12]. If there was any significant leakage around the membrane, it would be expected that this leakage term would dominate the salt passage data because the salinity of the feed is 25 to 100 times more saline than the permeate. If the leakage is the dominant force in the salt passage data, than it would be expected that the sodium sulfate and the sodium chloride salt passage results would be the same. Since they are clearly different, it can be determined that this setup will indeed measure permeability and salt passage through the membrane rather than around it.

3.2 Procedure

As stated at the beginning of this chapter, the three pressures that the membranes were tested under were 34.5 bar, 103.4 bar, and 172.4 bar. These pressures were picked to reflect the industry standard for reverse osmosis (RO) systems with this membrane (34.5 bar), the highest pressure the stirred cell could handle (172.4 bar) and a pressure in between these two pressures (103.4 bar). During the trials the pressure never fluctuated more than 10% from the specified pressure.

Once the lid was on the stirred cell, pressure was applied from the nitrogen gas cylinder using a pressure regulator. The first phase to complete was the beginning

salt passage phase. The process for this phase was:

1. The phase was allowed to run for 30 minutes in this state.
2. After 30 min, the collection container was removed and a new collection container was put under the output spigot.
3. The conductivity of this first container was measured and recorded. This conductivity was associated with the 1st 30 min section of this trial.
4. After 15 min, the pressure was released from the cell. The conductivity of the permeate in this collection cup was measured and recorded. This conductivity was associated with the 1st 15 minute section of the trial.

After the initial salt passage, the stirrer was removed from the cell and the remaining solution was emptied from the cell. The cell and the stirrer were rinsed with DI water. The cell was then filled with 300 mL of DI water and the stirrer was put back in the cell. The collection container at the output spigot of the cell was replaced and the stirrer was turned on to 500 rpm. The lid was closed and then the pressure was added back into the cell.

This phase of the trial lasted for 7 hours. Since the amount of feed that the cell can hold was much less than the flow through the membrane multiplied by 7 hours, the cell was refilled periodically. The process for refilling the cell was:

1. The pressure to the cell was released and the stirrer was turned off.
2. The lid was removed and DI water was added to fill the cell up to the 300 mL line.
3. The lid was replaced and the stirrer was turned back on.
4. The pressure to the cell was put back on.

At the end of the 7 hour long term permeability phase, the final salt passage phase was conducted. The process for switching from the long term permeability phase to the final salt passage phase was:

1. The pressure to the cell was released and the stirrer was turned off.
2. The lid and stirrer were removed from the cell.
3. The remaining DI water in the cell was removed.
4. 300 mL of a 1 g per 1 L of solution of NaCl was added to the cell.
5. The stirrer was replaced on the cell and the lid was reinstalled.
6. The pressure was put back on.
7. The remaining steps follow the same procedure as the initial salt passage phase.

At the end of the final salt passage phase the trial was considered complete. A complete list of times and steps taken for each test can be found in Tables 3.1 through 3.3 on pages 21 through 22.

3.3 Data Processing

During the trials, data was collected using a computer script that collected data from the mass scale every 5 seconds. To calculate the flux the total weight change of the cup was calculated over 750 second intervals and then divided by 750 seconds. In previous experiments nitrogen degassing through the stirred cell occurred approximately every 90 to 150 seconds, which would reduce the instantaneous flow rate of the stirred cell to 0 for about 5 seconds. In order to have a time-averaging of 5 to 10 times the period of this event, a 750 second interval was used to find the flux of the mass data.

The permeability was computed by dividing the water flux by the applied hydraulic pressure, adjusting for the osmotic pressure at the surface of the RO membrane during the salt passage phases.

$$A_m = \frac{J_w}{P - \pi e^{J_w/k}} \tag{3.2}$$

J_w is the water flux, A_m is the permeability of the membrane to water, π is the osmotic pressure of the solution and k is the mass transfer coefficient resulting from

stirring. All tests were operated with the stir bar rotating at 500 rpm, giving rise to an estimated mass transfer coefficient of 4×10^{-5} m/s $\pm 6\%$. The effective area of the membrane was taken to be 14.38 cm^2, determined via measurement with calipers of the o-ring inner diameter.

For the initial and final salt passage phases the equation used to calculate the apparent salt passage SP_a was:

$$SP_a = S_p/S_{f,o} \approx k_p/k_{f,o} \tag{3.3}$$

where k_p is the apparent permeate conductivity and $k_{f,o}$ is the initial feed conductivity.

This however is not entirely accurate because as the salt passage phase goes on the amount of feed decreases but the amount of salt in the feed stays the same. In order to correct for the increasing salinity in the feed, a corrective factor was added to the feed salinity.

$$SP = -\frac{k_p M_p(\tau)}{k_{f,o} M_{f,o} ln\left(1 - \frac{M_p(\tau)}{M_{f,o}}\right)} \tag{3.4}$$

where SP is the corrected salt passage through the membrane, k_p is the conductivity of the permeate, M_p is the mass of the permeate at time τ, $k_{f,o}$ is the original conductivity of the feed, and $M_{f,o}$ is the original mass of the feed. A proof for this corrective factor can be found in Appendix A.

SP_a and SP can therefore be related through the equation:

$$SP = -SP_a \frac{M_p(\tau)}{M_{f,o} ln\left(1 - \frac{M_p(\tau)}{M_{f,o}}\right)} \tag{3.5}$$

Finally, the conductivity of the feed at the beginning of the 15 minute salt passage phase was not measured and so must be calculated. Salt passage was taken as zero for this calculation. Thus:

$$k_{f,m} = \frac{k_{f,o} M_{f,o}}{M_{f,m}} \tag{3.6}$$

where $k_{f,m}$ is the conductivity of the feed at the beginning of the 15 min salt passage test, and $M_{f,m}$ is the mass of the solution in the cell at the beginning of the 15 min salt passage test. $M_{f,m}$ can be calculated using:

$$M_{f,m} = M_{f,o} - M_p(\tau) \tag{3.7}$$

where τ for Equation 3.7 is the time after the 30 min test.

3.4 Modeling

In literature, NF membranes follow a viscoelastic model which models the active layer via a spring and a damper that are connected in parallel. The proposed viscoelastic model for this RO membrane is similar:

$$PA = Kx + C\dot{x} \tag{3.8}$$

where P is the applied pressure in Pa, A is the area of the membrane in m^2, K is a spring constant in Pa, and C is a damper constant in Pa$\times$s. x is the active layer compaction, defined as the change in thickness from the original thickness. The solution to this equation takes the form:

$$x = \left(x' - \frac{PA}{K}\right) e^{-\frac{Kt}{C}} + \frac{PA}{K} \tag{3.9}$$

where x' is the initial level of compaction, which is zero at the beginning of the experiment, and t is the time elapsed. Essentially this equation predicts that when a constant pressure is applied, the strain will rise towards an asymptotic strain level. When there is no pressure, the strain will fall asymptotically to zero.

This experiment does not measure the compaction of the membrane; however it does measure the permeability and flux through the membrane. To relate compaction to permeability, we assume a linear relationship between the change in permeability and the strain, as indicated in Equation 3.10 [11].

$$1 - \frac{A_m}{A_m^o} = \frac{x}{\delta} \tag{3.10}$$

where A_m is the permeability of the membrane, A_m^o is the permeability measured after the initial application of pressure, and $\frac{x}{\delta}$ is the strain of the active layer. This equation can be rewritten as:

$$\frac{x}{\delta} = 1 - \frac{A_m}{A_m^o} \tag{3.11}$$

Multiplying 3.9 by $1/\delta$ and substituting in 3.11 we obtain:

$$A_m = A_m^o \left(1 - \frac{PA}{K\delta} + \left(\frac{PA}{K\delta} - \frac{x'}{\delta}\right) e^{-\frac{K\delta t}{C\delta}}\right) \tag{3.12}$$

Using equation 3.11 with x' as x, the equation for x'/δ becomes:

$$\frac{x'}{\delta} = 1 - \frac{A'_m}{A_m^o} \tag{3.13}$$

where A'_m is the initial permeability at time equals zero and x' is the initial compaction at time equals zero. This is notably different from A_m^o which is the permeability when the membrane experiences no compaction.

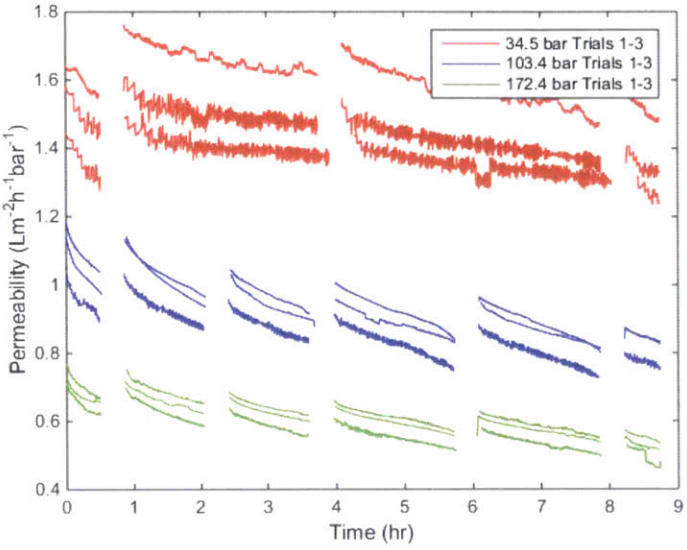

Figure 4-1: Graph showing permeability data for 3 different pressures.

at time t and t is measured in minutes. The results of this can be seen in Figures 4-2 through 4-4.

In these figures it appears that the 1st salt test for the 34.5 bar run always have a much lower permeability than the rest of the data. For 172.4 bar and 103.4 bar tests that does not seem to be an issue with the salt tests.

4.2 Salt Passage

Figure 4-6 illustrates salt passage through the membrane at various points during the 9-hour permeability tests. These salt passage tests were done at the beginning and end of the 9-hour permeability tests. The permeate salt concentration measurements were taken after the first 30 minutes and the next 15 minutes. In between these two measurements the permeate container was replaced.

As we can see in the 2nd 15 minute data, the salinity of the permeate is about 1% of the salinity of the feed. The SWC Membrane data sheet specifies that in an industrial setting the membrane has about 99.7% salt rejection. These tests indicate rejection of 99%, which is 0.7% below the specification sheet. There are multiple

Chapter 4

Results/Discussion

4.1 Permeability

In Figure 4-1 we can see the permeability of the membrane at three different pressures. As time goes on we can see the permeability of the membranes decrease steadily. The discontinuities in the chart are due to the liquid in the stirred cell being replaced. Before the first discontinuity an NaCl solution was in the stirred cell for a salt rejection test. After the last discontinuity an NaCl solution was also in the cell. While conducting the salt passage phases, the pressure used the calculate the permeability was the osmotic pressure at the surface of the membrane as seen in Equation 3.2.

The difference between different trials within a test can be attributed to both measurement error and slight differences in membrane properties. However, the measurement error for permeability is only approximately 1%, and the differences between trials seems to be much greater than that. Therefore most of the error can be attributed purely to inconsistencies between membranes. To negate this error, the data is normalized to the last 8 min of the long permeability phase using the following equation:

$$A_{m,n}(t) = \frac{A_m(487) - A_m(479)}{8} \tag{4.1}$$

where $A_{m,n}(t)$ is the normalized permeability at time t, $A_m(t)$ is the permeability

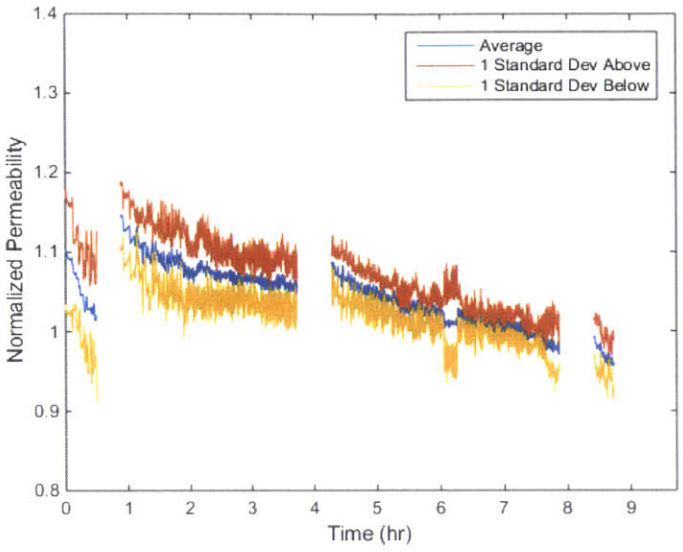

Figure 4-2: Averaged Normalized Permeability Data for 34.5 bar

reasons why this might be the case. The first is that this specification is assuming the membrane is used in an industrial-scale reverse osmosis plant, whereas we are using it on a laboratory scale. Another reason is that the specification is made for a perfect membrane, however as we see in the permeability data and later in the salt passage data, the membranes are inconsistent between one membrane sample and the next.

In Figure 4-6 we can see that the initial salt tests had much more variation than the final salt tests. The error of the data is too large to determine whether or not salt passage is correlated with pressure. As in permeability, the error in measurement between tests is small (about 3% due to conductivity meter measurement variations) and does not explain the large variance between tests. Thus to better compare tests, the results were normalized to the final 15 minutes in Figure 4.2.

From our data we found that the sodium sulfate salt passage tests turned up a much lower concentration than the sodium chloride solution and so we can discount leakage as a factor of error in our results (see Section 3.1.1 for an in depth explanation). In Appendix B uncorrected and corrected salt passage data for each run can be found.

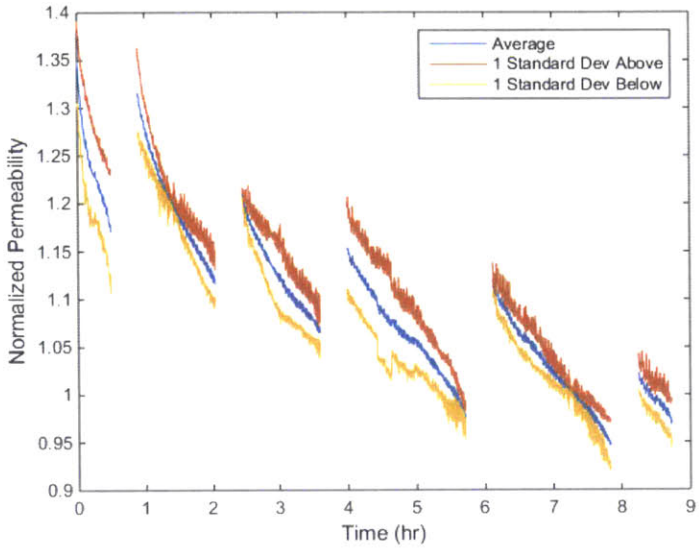

Figure 4-3: Averaged Normalized Permeability Data for 103.4 bar

4.3 Modeling

The corrected permeability data was fit with the viscoelastic model solved in Section 3.4. In this model, P and A were known, A_m^o was measured as the initial permeability for each test. A'_m was an initial condition that was recalculated for every phase (every time the pressure changed), and t was restarted at these points as well. For the first phase, $A_m^o = A'_m$; for subsequent phases, A'_m was the permeability at the end of the previous phase. The model was then fit to the test data by adjusting the values of $C\delta$ and $K\delta$. The δ term was left in the spring constant and damping constant because the initial thickness of the active layer was not measured in these experiments. In Figures 4-7 through 4-9 are charts of a representative trial of each test with permeability data and with a fit line. The complete collection of fit data can be found in Appendix C. From these figures it can be seen that this visco-elastic model is a good fit when describing the overall strain shape of the membrane. However, at each pressure initiation this model does not quite capture the short-term permeability decrease of the membrane nor the permeability recovery of the membrane.

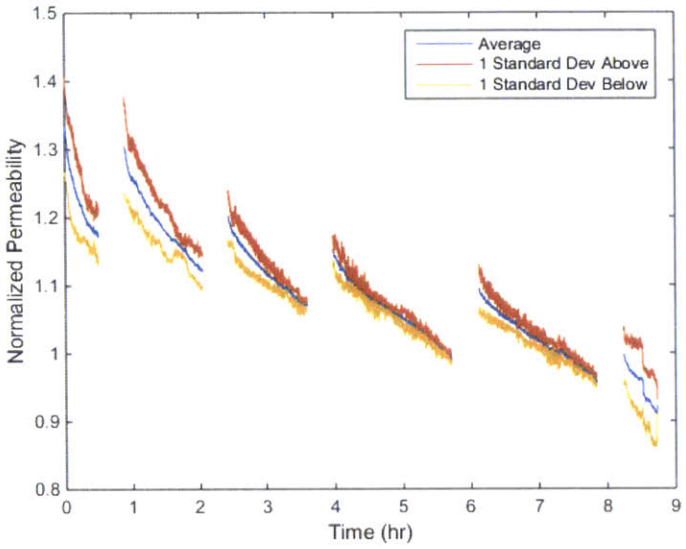

Figure 4-4: Averaged Normalized Permeability Data for 172.4 bar

Trial Number	Pressure	$C\delta$ (MPa m^2 s)	$K\delta$ (Pa m^2)
Trial 1	34.5 bar	480	28000
Trial 2	34.5 bar	480	21000
Trial 3	34.5 bar	480	28000
Trial 1	103.4 bar	450	45000
Trial 2	103.4 bar	340	45000
Trial 3	103.4 bar	340	450000
Trial 1	172.4 bar	830	62000
Trial 2	172.4 bar	760	69000
Trial 3	172.4 bar	760	83000

Table 4.1: Table of the $C\delta$ and $K\delta$ values for each trial.

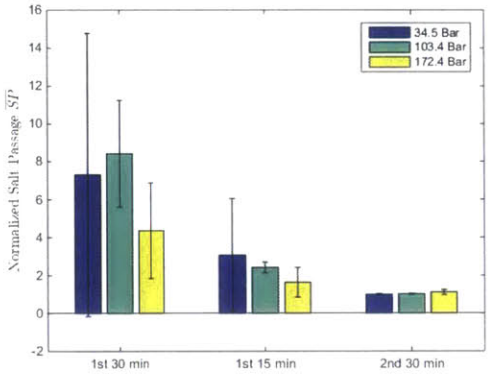

Figure 4-5: Corrected and normalized salt passage data for each test averaged over their trials including standard deviation bars representing 2 standard deviations.

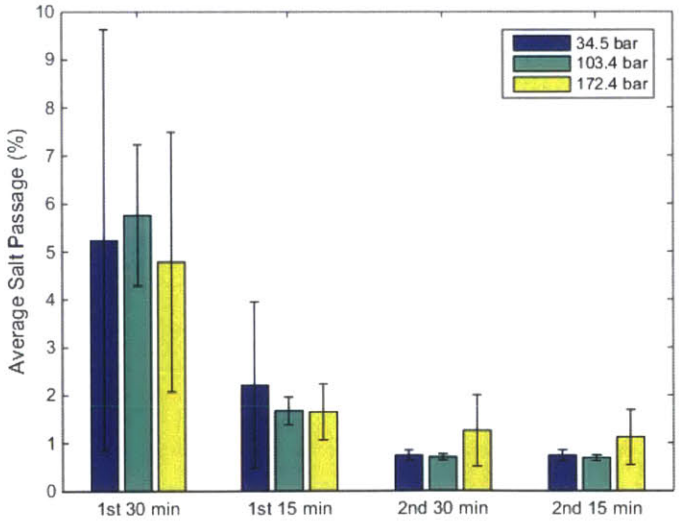

Figure 4-6: Bar graph representing the average salt passage for each pressure (corrected but not normalized)

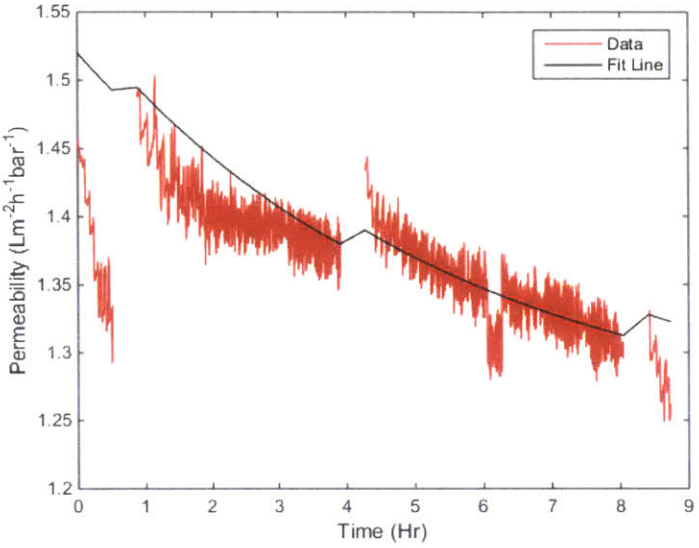

Figure 4-7: The data from a 34.5 bar trial and a viscoelastic model with a spring and damper in parallel.

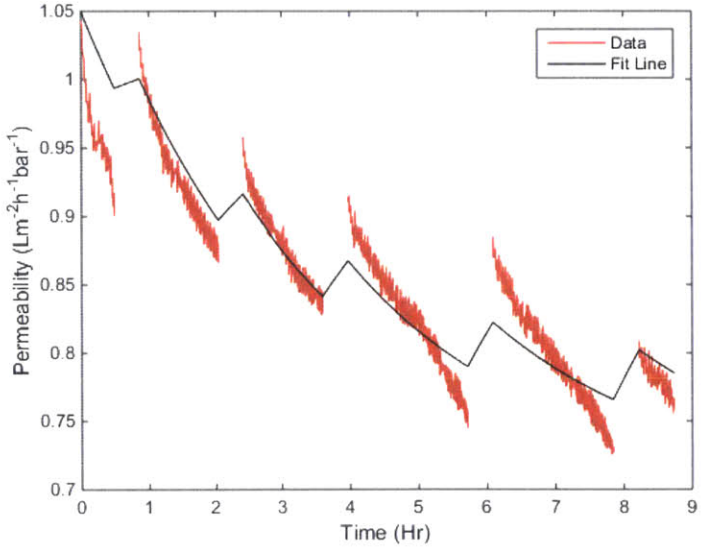

Figure 4-8: The data from a 103.4 bar trial and a viscoelastic model with a spring and damper in parallel.

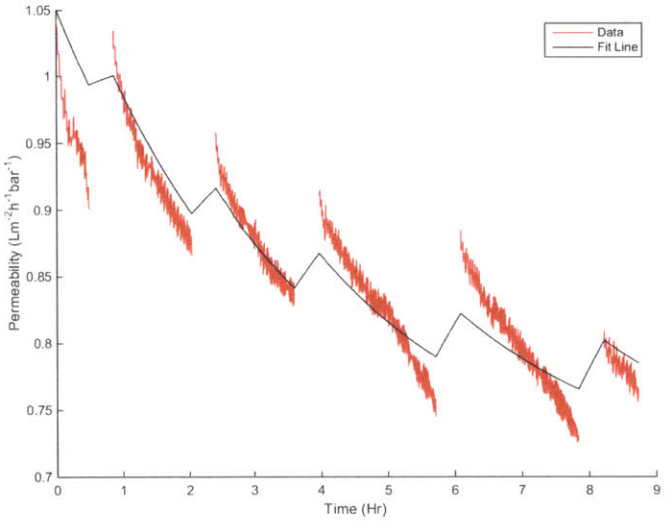

Figure 4-9: The data from a 172.4 bar trial and a viscoelastic model with a spring and damper in parallel.

Chapter 5

Conclusion

In this experiment it was determined that the salt passage of the membrane at pressures of 172 bar was very similar to the salt passage of the membrane at 34.5 bar, showing that salt passage does not increase as the pressure increases to 172 bar. It was also shown that at 172 bar the permeability of the membrane fell to 50% of its permeability at 34.5 bar. Through modeling it was shown that a simple viscoelastic model was able to be used to achieve the overall shape of the permeability data for the tests run. The model, however, is not able to capture the recovery of permeability when the pressure is removed.

The potential benefits, especially in terms of reduced energy consumption, of replacing technologies such as mechanical vapor compression with high pressure reverse osmosis are very significant. We can therefore believe that high pressure reverse osmosis holds great promise for the near future.

Appendix A

Corrected Salt Passage

Salt passage can be described by:

$$SP = k_p/k_f \approx S_p/S_f \tag{A.1}$$

where SP is salt passage, k_p is conductivity of the permeate, k_f is the conductivity of the feed, S_p is the salinity of the permeate and S_f is the salinity of the feed, where salinity is described as solute divided by solution. From this:

$$S_p = SP \times S_f \tag{A.2}$$

From the definition of salinity and assuming that salt passage is zero to first order:

$$M_{f,o}S_{f,o} = M_f(t)S_f(t) \tag{A.3}$$

where $M_{f,o}$ is the original mass of the feed, $S_{f,o}$ is the original salinity of the feed, $M_f(t)$ is the mass of the feed at a point in time and $S_f(t)$ is the salinity of the feed at the same point in time.

If $M_p(t)$ is the mass of the permeate at time t, then from the above equations:

$$M_f(t) = M_{f,o} - M_p(t) \tag{A.4}$$

Substituting A.4 into A.3 and solving for $S_f(t)$:

$$S_f(t) = \frac{M_{f,o}}{M_{f,o} - M_p(t)} S_{f,o} \tag{A.5}$$

Substituting A.5 into A.2:

$$S_p = SP \frac{M_{f,o}}{M_{f,o} - M_p(t)} S_{f,o} \tag{A.6}$$

The function $M_p(t)$ can be described by:

$$M_p(t) = \dot{M}_p t \tag{A.7}$$

The average salinity $\overline{S_p}(t)$ over a period of time from t = 0 to t = t:

$$\overline{S_p}(t) = \frac{\int_0^\tau S_p \dot{M}_p \, \mathrm{d}t}{M_p(\tau)} \tag{A.8}$$

where $\dot{M}_p$ is the mass flux of the permeate.

Substituting A.7 into A.6 and substituting the result into A.8 and assuming constant $\dot{M}_p$:

$$\overline{S_p}(t) = \dot{M}_p / M_p(t) \int_0^\tau SP \frac{1}{1 - \frac{M_p}{M_{f,o}}} S_{f,o} \, \mathrm{d}t \tag{A.9}$$

Integrating from 0 to τ:

$$\overline{S_p}(t) = \frac{-M_{f,o}}{M_p(\tau)} SP \times S_{f,o} ln\left(M_{f,o} - \dot{M}_p(\tau)\right) \tag{A.10}$$

Rearranging A.10 and solving for SP:

$$SP = -\frac{\overline{S_p}(\tau)}{S_{f,o}} \frac{M_p(\tau)}{M_{f,o}} \frac{1}{ln\left(M_{f,o} - \dot{M}_p \tau\right)} \tag{A.11}$$

From A.1 the conductivities can be substituted for salinities in A.11 and Equation A.7 can be substituted in for $\dot{M}_p \tau$:

$$SP = -\frac{\overline{k_p}(\tau)}{k_{f,o}} \frac{M_p(\tau)}{M_{f,o}} \frac{1}{ln\left(M_{f,o} - M_p(\tau)\right)} \tag{A.12}$$

Appendix B

Salt Passage Data

In figure B the salt passage data for each salt passage phase of each trial was normalized by the final salt passage phase of that trial. For example, for the 34.5 bar tests, for Trial 1 the initial 30 min salt passage data was divided by the final 15 min salt passage data for Trial 1 of the 34.5 bar tests.

Since there may be slight differences between each membrane used, normalization was necessary in order to negate these differences in membranes. This was done in order to give an idea of the experimental error excluding the effects of membrane differences.

Salt passage is lower when corrected in each instance. This is due to uncorrected salt passage calculated by dividing the permeate conductivity by the feed conductivity before the first 30 minute test. As the test transpires, the feed conductivity increases. This increase is captured by the corrected salt passage, and so corrected salt passage is less than uncorrected salt passage.

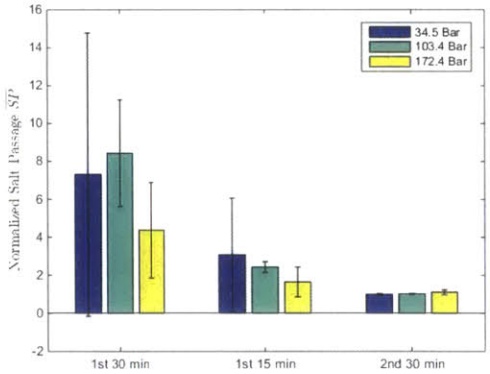

Figure B-1: Corrected and normalized salt passage data for each test averaged over their trials including standard deviation bars representing 2 standard deviations.

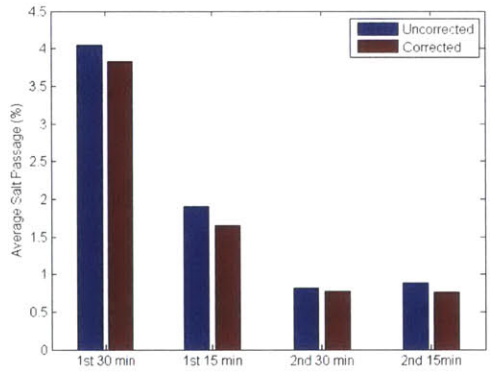

Figure B-2: Uncorrected and corrected salt passage data for the first trial of 34.5 bar

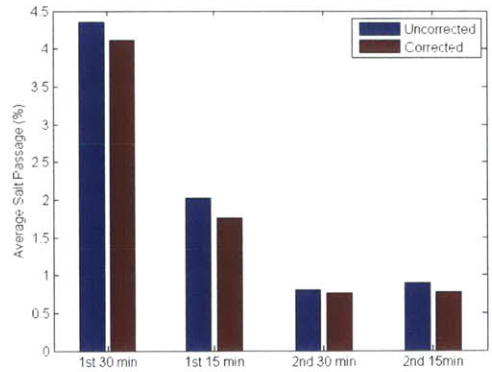

Figure B-3: Uncorrected and corrected salt passage data for the second trial of 34.5 bar

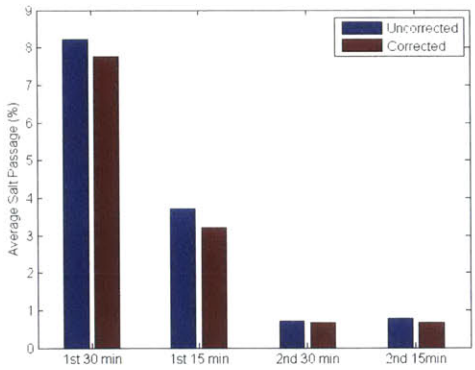

Figure B-4: Uncorrected and corrected salt passage data for the third trial of 34.5 bar

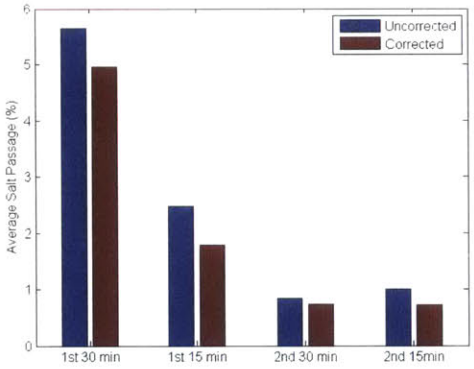

Figure B-5: Uncorrected and corrected salt passage data for the first trial of 103.4 bar

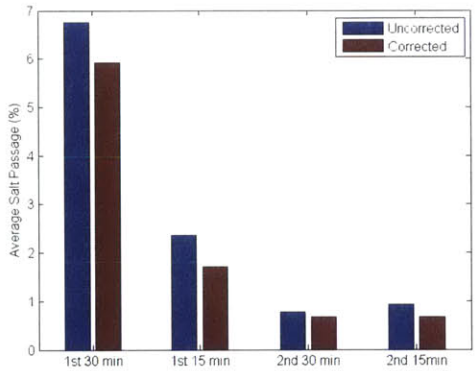

Figure B-6: Uncorrected and corrected salt passage data for the second trial of 103.4 bar

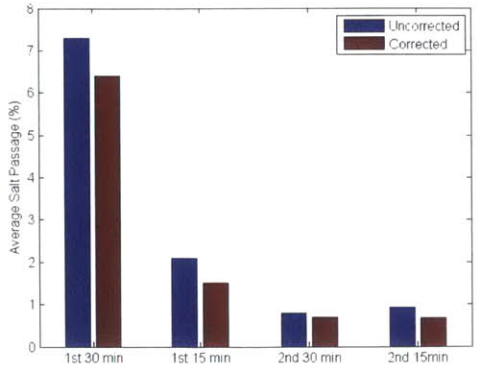

Figure B-7: Uncorrected and corrected salt passage data for the third trial of 103.4 bar

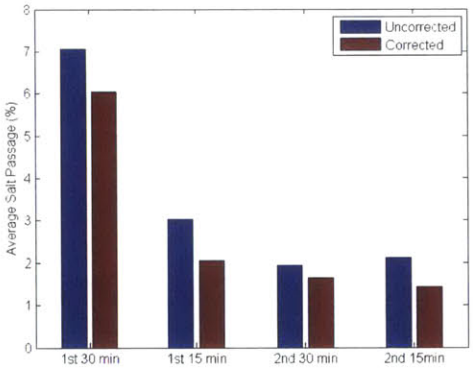

Figure B-8: Uncorrected and corrected salt passage data for the first trial of 172.4 bar

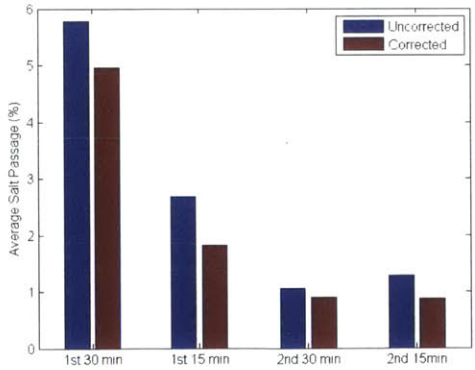

Figure B-9: Uncorrected and corrected salt passage data for the second trial of 172.4 bar

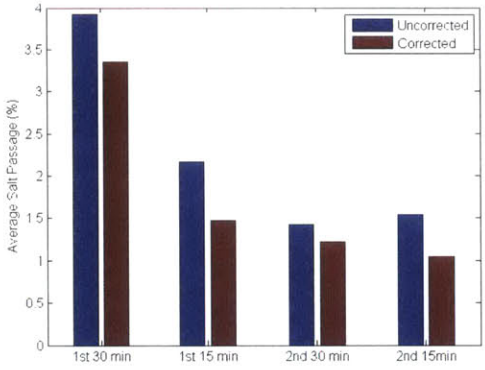

Figure B-10: Uncorrected and corrected salt passage data for the third trial of 172.4 bar

Appendix C

Permeability with Fit Lines

Here are the complete graphs with lines of best fit for every trial done. This includes graphs already presented in the Results section as well as the additional two trials for each pressure test.

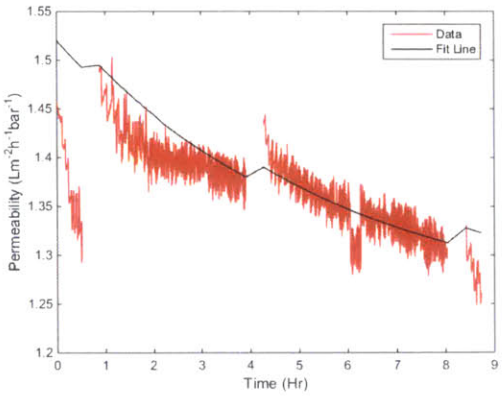

Figure C-1: Fit line with data for Trial 1 of the 34.5 bar test.

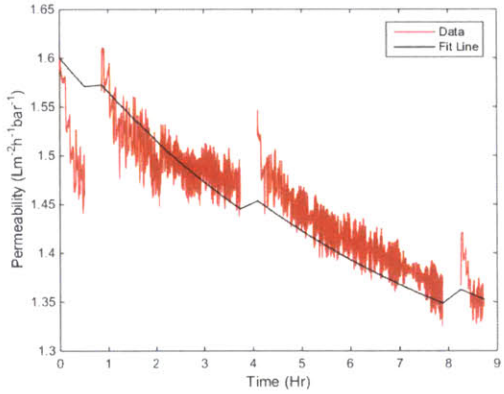

Figure C-2: Fit line with data for Trial 2 of the 34.5 bar test.

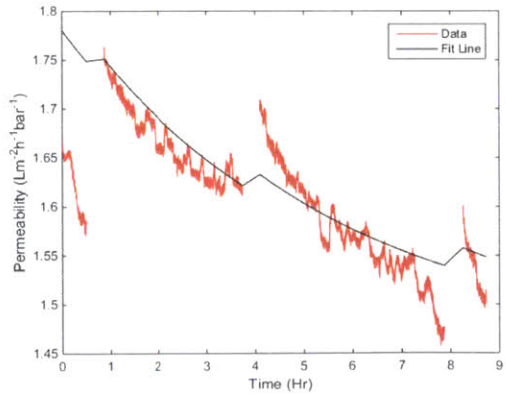

Figure C-3: Fit line with data for Trial 3 of the 34.5 bar test.

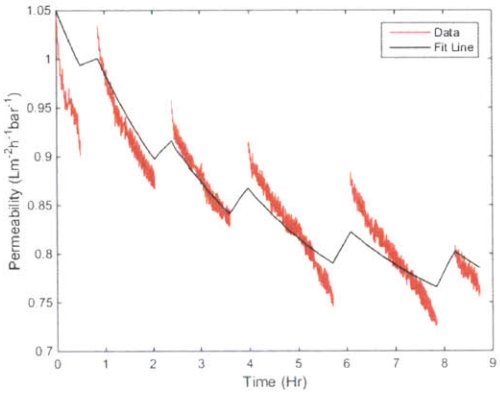

Figure C-4: Fit line with data for Trial 1 of the 103.4 bar test.

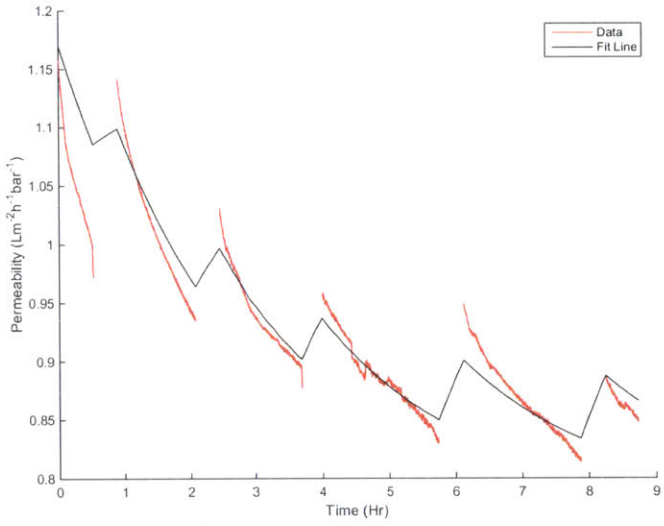

Figure C-5: Fit line with data for Trial 2 of the 103.4 bar test.

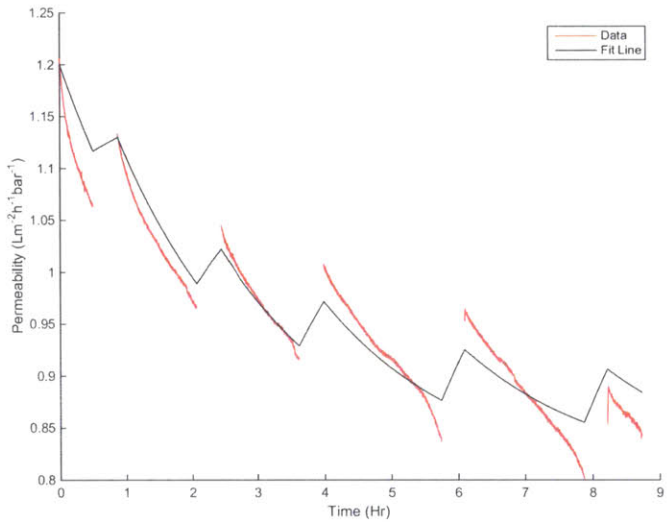

Figure C-6: Fit line with data for Trial 3 of the 103.4 bar test.

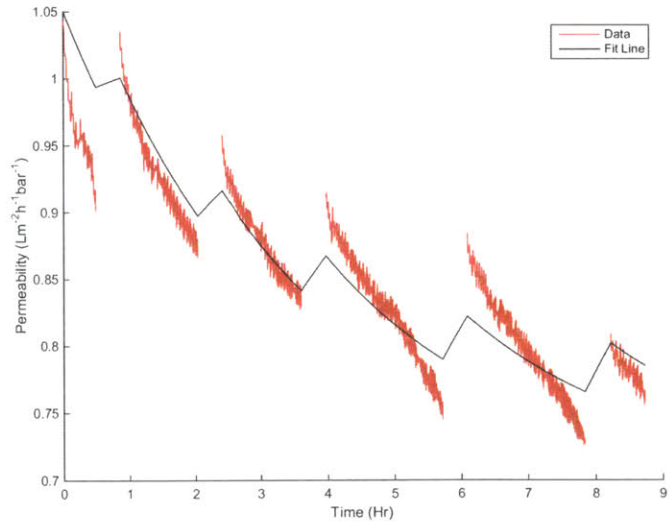

Figure C-7: Fit line with data for Trial 1 of the 172.4 bar test.

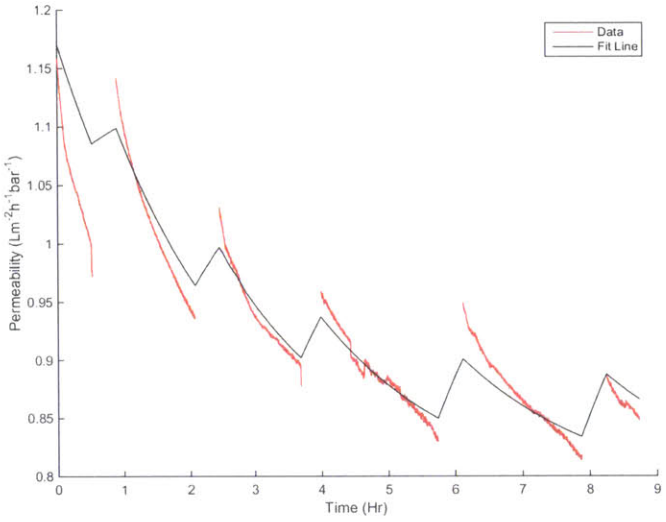

Figure C-8: Fit line with data for Trial 2 of the 172.4 bar test.

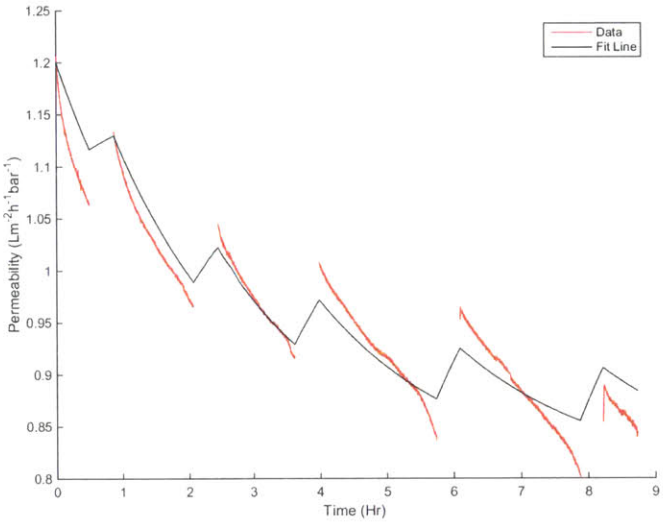

Figure C-9: Fit line with data for Trial 3 of the 172.4 bar test.

Appendix D

Stirred Cell Setup Details

This section goes through the details of running this stirred cell apparatus at MIT in Professor Anand's laboratory. This procedure assumes that the pressure line is already setup and that the data collection apparatus is already setup.

D.0.1 Parts List

- HP4750X Stirred Cell, Sterlitech, Washington, USA
- 1/4" Hex Key Head Torque Wrench, McMaster-Carr, New Jersey, USA. Part Number 5347A155
- Steam-Resistant EPDM O-Ring, 1/8 Fractional Width, Dash Number 222, McMaster-Carr, New Jersey, USA, Part Number 9557K492
- Bostik "Never-Seez" Anti-Seize and Lubricating Compound. McMaster-Carr, New Jersey, USA, Part Number 1820K23
- Oil Filter Wrench. Economy Hardware, 438 Massachusetts Avenue, Cambridge, MA.
- 1/4" Long Hex L-Key. McMaster-Carr, New Jersey, USA. Part Number 7122A94
- DI Water, McMaster-Carr, New Jersey, USA. Part Number 3190K731

D.0.2 Procedure

Here are the procedures I used, as well as a few trouble-shooting hints, in order to ensure the HP4750X stirred cell properly worked. The definition of properly working was defined in Experimental Setup Validation in the Methods chapter. The main component of this working properly is ensuring that there is no or little leakage between the o-ring and the membrane.

The steps are as follows:

1. Rinse the stirred cell in water (this can be tap or DI water)

2. Connect lid to the pressure line (lid is 1/4" FNPT) using Teflon tape. This should be tightened with a wrench. It should be tightened more if leaks are heard once pressure is applied.

3. Cut out the membrane from the membrane sheet using the porous plate as a template.

   (a) Regular scissors for cutting paper should work. If the membrane doesn't cut similarly to printer paper then the scissors used might be dull and should be replaced.

   (b) Gloves should be worn whenever touching the active layer of the membrane. In this experiment with SWC membranes the active layer was shinier than the supporting structures. Care should also be taken that the active layer doesn't touch any other surface, as oils can degrade the active layer and other surfaces can scratch it.

4. Rinse the porous plate and the membrane in DI water to clear it of the solution that it was soaking in.

   (a) The membranes should be kept in a 1% sodium bisulfite solution to prevent things from growing in the container while it is stored.

(b) SWC membranes come packaged in liquid; however, some membranes are not and it was found that the length of time the membrane soaked in liquid before being used greatly affected its permeability.

5. Put in a new EPDM o-ring into the inverted stirred cell apparatus and wet the o-ring with DI water.

   (a) Extensive testing was not done as to whether it is necessary to replace the o-ring each time; however it seemed to produce slightly better results when we replaced it.

6. Place the membrane on top of the EPDM o-ring, active layer down (touching the o-ring). It should rest flat and shouldn't be squished by the edges of the stirred cell. If it is constrained by the edges of the stirred cell it could bend and fold when the bottom cap is put on.

7. Put porous metal plate on top of the membrane.

8. Put in the bottom of the cell on and screw it in. The bolts should be tightened to 20 ft/lbs.

   (a) To ensure that the bolts don't seize, apply anti-seize to the threads. This will allow the bolts to screw in more easily.

   (b) To get enough leverage to tighten the bolts to 20 ft/lbs, use a oil-filter wrench to hold the stirred cell.

   (c) If the oil-filter wrench starts slipping, use soapy water to wash the outside of the cell and then dry the cell. This was found to work very well to get the oil-filter wrench gripping the cell again. Do not get the soapy water inside the cell.

9. Put in liquid and stirring bar into the cell as needed.

10. Put on the top lid with the rubber gasket and tighten the bolts. (These can bet tightened using the hex l-key, no need to tighten to a certain torque specification or use the oil-filter wrench).

11. Cell is now ready to filter.

Bibliography

[1] Rektor, Atilla, Aron Kozak, Guyula Vatai, and Erika Bekassy-Molnar. "Pilot Plant RO-Filtration of Grape Juice." *Separation and Purification Technology* 57.3 (2007): 473-475.

[2] Baxter, A. G., M. E. Bednas, T. Matsuura, and S. Sourirajan. "Reverse Osmosis Concentration of Flavor Components in Apple Juice-and Grape Juice-Waters." *Chemical Engineering Communications* 4 (1980): 471-83.

[3] Gurak, Poliana D., Rosires Deliza, Lourdes M. Correa-Cabral, Maria H. Rocha-Leao, and Daniela G. Castro-Freitas. "Concentrated Grape Juice by Reserve Osmosis." *Agro FOOD Industry Hi Tech* 43.3 (2013): 37-39.

[4] Thiel, Gregory P., Emily W. Tow, Leonardo D. Banchik, Hyung Won Chung, and John H. Lienhard. "Energy consumption in desalinating produced water from shale oil and gas extraction." Desalination (2015).

[5] Stokes, R.H. "Appendix 8.10: Osmotic Coefficients of Electrolytes at 25°C." *Electrolyte Solutions, the Measurement and Interpretation of Conductance, Chemical Potential, and Diffusion in Solutions of Simple Electrolytes.* By Robert A. Robinson. 2nd ed. London: Butterworths, 1959. 483.

[6] Nabetani, Hiroshi, Mitsutoshi Nakajima, Atsuo Wtanabe, Shi-ichi Nakao, and Shoji Kimura. "Prediction of the Flux for the Reverse Osmosis of a Solution Containing Sucrose and Glucose." *Journal of Chemical Engineering of Japan* 25.5 (1992): 575-80.

[7] Ohya, Haruhiko. "An Expression Method of Compaction Effects on Reverse Osmosis Membranes at High Pressure Operation." *Desalination* 26 (1978): 163-74.

[8] Hussain, Yazan A., and Mohammed H. Al-Saleh. "A Viscoelastic-based Model for TFC Membranes Flux Reduction during Compaction." *Desalination* 344 (2014): 362-70.

[9] Hussain, Yazan A., and Mohammed H. Al-Saleh, and Suekainah S. Ar-Ratrout. "The effect of active layer non-uniformity on the flux and compaction of TFC membranes." *Desalination* 328 (2013): 17-23.

[10] Luk-Cyr, Jacques. *Experiments and modeling of multilayered coatings and membranes: application to thermal barrier coatings and reverse osmosis membranes*. SM Thesis. Massachusetts Institute of Technology, 2014.

[11] Vand Der Velden, P.M., and C. A. Smolders. "Initial flux decline and initial rejection increase for swollen ionic membranes." *Journal of Applied Polymer Science* 20.5 (1976): 1153-64.

[12] Meihong, Liu, Yu Sanchuan, Zhou Yong, Gao Congjie. "Study on the thin-film composite nanofiltration membrane for the removal of sulfate from concentrated salt aqueous: Preparation and performance." *Journal of Membrane Science* 310 (2008): 289-95.